Protein Science (1994), *3*:638–649. Cambridge University Press. Printed in the USA.

Slow-folding kinetics of ribonuclease-A by volume change and circular dichroism: Evidence for two independent reactions

JOEL A. YBE[1] AND PETER C. KAHN

Department of Biochemistry and Microbiology, Cook College, Rutgers University, New Brunswick, New Jersey 08903-0231

(RECEIVED November 10, 1993; ACCEPTED February 2, 1994)

Abstract

The slow refolding of guanidine-HCl-denatured ribonuclease-A was studied by volume change and by kinetic CD at 222 and 276 nm. Dilatometric measurements revealed that on refolding there is a fast volume change of +232 mL/mol of protein. This is followed by a very slow nonexponential change that takes about 25 min to reach equilibrium. By adding varying amounts of $(NH_4)_2SO_4$, the slow volume change curve was resolved into 2 concurrent reactions. The faster of the 2 slow events entails a negative volume change of −64 mL/mol of protein and appears to arise from proline isomerization. The slower process, attended by a positive change of +53 mL/mol of protein, has properties consistent with the "XY" reaction of Lin and Brandts (1983, *Biochemistry 22*:563–573). This reaction is so named because the conformational nature of neither its initial (Y) nor its final state (X) is known; the transition is characterized solely by its absorbance and fluorescence kinetics. These are the first direct physical measures attributable to the "XY" process. The early formation of a compact structure in the event responsible for the rapid +232-mL/mol volume change, however, is consistent with the sequential model of folding (Cook KH, Schmid FX, Baldwin RL, 1979, *Proc Natl Acad Sci USA 76*:6157–6161; Kim PS, Baldwin RL, 1980, *Biochemistry 19*:6124–6129). The usefulness of volume change measurements as a method of detecting structural rearrangements was confirmed by finding agreement between time constants obtained from parallel volume change and kinetic CD experiments. The measured volume changes arise from both changes in hydration and changes in the packing of atoms in the interior of the protein.

Keywords: circular dichroism; protein folding; protein hydration; ribonuclease-A; volume change

Understanding how particular amino acid sequences lead to the formation of unique biologically active structures remains a major challenge. Although the detailed mechanism of protein folding has yet to be resolved, the many in vitro studies on monomeric globular proteins suggest that the development of native structure can be, more or less, divided into 3 stages (Matthews, 1991). In the first stage of folding, which is complete in milliseconds, collapsed structures have been observed, some of which, at least, have properties of the "molten globule" (Kuwajima et al., 1976; Sugawara et al., 1991). The rapid formation of secondary structure in this stage is borne out by experiments combining pulsed-labeling hydrogen-exchange and high-resolution NMR spectroscopy; a significant fraction of the amide hydrogens in cytochrome *c* (Roder et al., 1988) and barnase (Bycroft et al., 1990) are protected from exchange in the first 1–4 ms of refolding. In the middle stage of folding, stable supersecondary structures begin to coalesce. Hydrogen-exchange experiments on ribonuclease-A (Udgaonkar & Baldwin, 1988), cytochrome *c* (Roder et al., 1988), and barnase (Bycroft et al., 1990) indicate that tyrosine and tryptophan residues become buried in this step. There is abundant evidence that suggests the sequential formation of 3-dimensional structure (see, for example, Baldwin, 1993). This supports the framework model (Kim & Baldwin, 1982, 1990), which supposes that an intermediate with native or nearly native secondary structure is formed before tertiary structure is locked in place. However, there is mounting evidence that multiple folding pathways are also accessible to proteins (Harrison & Durbin, 1985; Gittelman & Matthews, 1990; Kuwajima et al., 1991; Radford et al., 1992; Wilkins et al., 1993).

In the last stage of structure development, final adjustments to the tertiary structure are made, and the fully native conformation emerges. In general, the rate-limiting step occurs at this stage (Brandts et al., 1975). For proteins with proline residues, the rate-limiting step is often *cis–trans* proline isomerization. A

Reprint requests to: Peter C. Kahn, Department of Biochemistry and Microbiology, 328 Lipman Hall, Cook College, Rutgers University, New Brunswick, New Jersey 08903; e-mail: kahn@biovax.rutgers.edu.

[1] Present address: Department of Chemistry, Frick Laboratory, Princeton University, Princeton, New Jersey 08544-1009.

Abbreviations: AMS, ammonium sulfate; GuHCl, guanidine hydrochloride; ISP, isomer-specific proteolysis; RNase-A, ribonuclease-A.

well-studied example is the refolding of RNase-A, which is complicated by the presence of fast- and slow-folding species in a 1:4 proportion (Garel & Baldwin, 1973; Garel et al., 1976). The folding of RNase-A is further complicated by an additional slow kinetic phase observed under some refolding conditions (Schmid, 1981; Lin & Brandts, 1983c). Although the fast-folding species refold in milliseconds, the slow-folding species require minutes to become native. The proline hypothesis (Brandts et al., 1975) offers that refolding is slow because X-Pro peptide bonds, which become non-native as a result of unfolding, must convert back to their correct configurations—an inherently slow event—before the protein can become native.

Much effort has gone into identifying the residues responsible for slow folding in RNase-A, including comparative kinetic studies on RNases from a variety of sources (Schmid et al., 1986) and the development of the isomer-specific proteolysis (ISP) method to probe directly the configuration of X-Pro peptide bonds in denatured RNase-A (Lin & Brandts, 1983a, 1983b, 1984). The ISP studies yielded an unexpected result: most of the slow-folding amplitude appeared not to be proline limited. Instead, 50% of the total amplitude arose from a reaction with properties decidedly different from those of *cis–trans* proline isomerization (Lin & Brandts, 1983c, 1983d). Firstly, the rate of the reaction was much slower than expected of proline isomerization. Secondly, the activation enthalpy of the event was smaller than that of *cis–trans* proline isomerization. Thirdly, the rate of the event was strongly dependent on ammonium sulfate and guanidine hydrochloride concentrations, which is uncharacteristic of proline isomerization (Schmid, 1981; Lin & Brandts, 1983c). Finally, the kinetic phase was not accelerated by *cis–trans* prolyl isomerase (Lin & Brandts, 1984). Recently, Adler and Scheraga (1990) presented data indicating that the slow amplitude can be fully accounted for by proline isomerization. However, the nature of the discrepancy between their results and the results of the ISP studies is unknown (Schultz et al., 1992).

Most workers now agree that there are 2 slow kinetic phases in the refolding of RNase-A (Schmid, 1981; Lin & Brandts, 1983c, 1988). However, they disagree on the nature of the molecular events that give rise to these phases. There is a view that both slow kinetic phases are explained by *cis–trans* proline isomerization (Cook et al., 1979; Schmid, 1983, 1986). Alternatively, there is a view that *cis–trans* proline isomerization is only a minor component of the slow-folding amplitude; the major component is a new slow reaction (named the "XY" process by Lin & Brandts) whose kinetic properties, described above, are very different from those of proline isomerization. To clarify the nature of the slow events in the refolding of RNase-A, we have followed the refolding reaction by volume change. Volumetric changes occur on refolding primarily because apolar side chains exposed to bulk water in the unfolded form are transferred into the hydrophobic interior of the folded protein (Kauzmann, 1959; Cooke & Kuntz, 1974; Kuntz & Kauzmann, 1974). The expulsion into the bulk solvent of water of hydration, whose density changes in the process, gives rise, in part, to the volumetric effects. It is hoped that different unfolded forms will exhibit different volumetric properties upon folding. This would be useful in telling them apart, because they cannot be distinguished on the basis of their spectroscopic properties alone (Brandts et al., 1975).

To verify that changes in volume are the direct result of structural rearrangements, the refolding reactions followed by volume change were also monitored by CD in both the near- and far-UV. This method has been used previously to follow the folding kinetics of a number of proteins including lysozyme, α-lactalbumin, parvalbumin (Kuwajima et al., 1985, 1987, 1988), and staphylococcal nuclease A (Sugawara et al., 1991). Solution conditions which destabilize intermediates and yield first-order folding kinetics when examined by spectroscopic methods were adopted in order to relate the present work to prior studies which suggested that the slow kinetic phase was due entirely to proline isomerization (Schmid & Baldwin, 1978; Cook et al., 1979; Schmid, 1983, 1986; Schmid et al., 1986).

We report that RNase-A refolding is accompanied by a fast positive volume change arising from the rapid formation of compact structures in the early stages of folding. This is followed by a slow negative volume change, which proceeds with a time constant typical of *cis–trans* proline isomerization reported under similar experimental conditions. In addition, a very slow positive volume change is seen whose rate is strongly accelerated by AMS. We offer evidence that this volume change is not due to proline isomerization. The accompanying CD experiments indicate that the observed slow volume changes arise from both secondary and tertiary structural changes, which occur in a concerted fashion.

Results

Volume change of refolding

Figure 1 shows the average of 3 volume-change experiments in the absence of AMS. A rapid increase in volume change, ΔV_{fast}, was observed within the mixing dead time of 1–2 min.

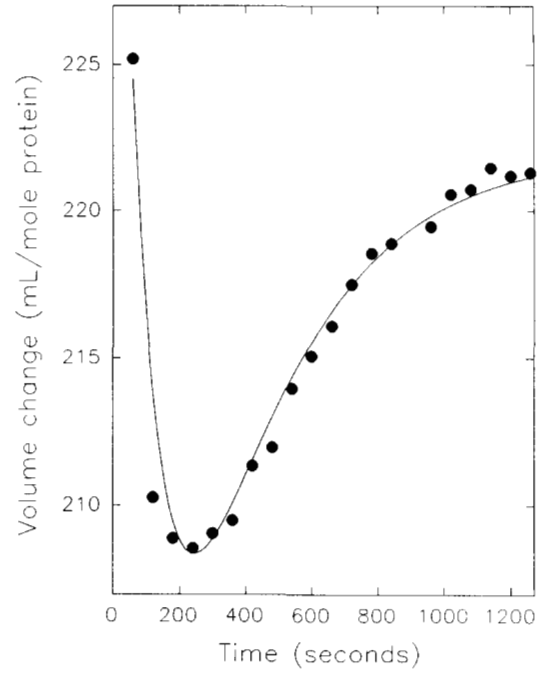

Fig. 1. Time dependence of the slow volume change of RNase-A refolding in the absence of $(NH_4)_2SO_4$. Protein concentration was 20 mg/mL (1.46 mM). Denaturing conditions: 3 M GuHCl, 40 mM histidine, pH 2. Renaturing conditions: 2.5 M GuHCl, 33 mM histidine, pH 6.5–7. The fitted curve, calculated as in the text, is shown as a solid line.

The fast rise was followed by a nonexponential change which took about 25 min to reach equilibrium.

The absorbance kinetics of the slow-folding reaction can be altered by simply adding AMS (Schmid, 1981; Lin & Brandts, 1983c). The effect of this additive on the complex nonexponential volume change is shown in Figure 2. The results of nonlinear regressions to the data are presented in Table 1. As the AMS concentration rises from 0 to 0.52 M, the complex volume change was reduced to a single first-order decrease in volume. Raising the concentration of AMS to 0.2 M decreased the size of the negative volume change from −63.5 ± 9.8 mL/mol of protein to −47.9 ± 0.4 mL/mol of protein. The negative volume change did not change significantly from 0.2 to 0.52 M AMS. The diminution in the negative volume change in the range up to 0.2 M AMS is attended by a decrease in the slow positive volume change from +53.1 ± 6.7 to +41.7 ± 1.1 mL/mol of protein. The slow positive volume change is completely lost in the presence of 0.52 M AMS. Experiments at 0.35 M AMS yield the same results as at 0.52 M (data not shown).

Raising the AMS concentration also accelerated the rate of the slow positive change. Upon the addition of 0.2 M AMS, the rate of the positive volume change was increased, the relaxation time falling from 293 ± 17 to 191 ± 12 s. The largest rate enhancement was observed at AMS concentrations ≥0.35 M, going from 293 ± 17 s in the absence of AMS to a value too small to be measured in the manually mixed experiments.

Enhancing the rate of the positive volume change should displace a fraction of the event into the dead time of mixing. This is evident in Figure 2. As the AMS concentration rose from 0 to 0.2 M, ΔV_{fast} increased from +232 ± 13 to +252 ± 11 mL/mol of protein. The observed increase in ΔV_{fast} of +20 mL/mol of protein agrees well with the expected net increase of +27 mL/mol of protein from the net change in amplitude of the 2 slow events (see Table 1). Apparently other volumetric effects must be considered when the AMS concentration exceeds 0.2 M because the observed increase in ΔV_{fast} in this AMS range is smaller than the sum of changes in the slow events. Nonspecific association of AMS is a possible contributor here.

In contrast to the dramatic effect of AMS on the rate of the positive volume change, the additive did not change the rate of the negative volume change nearly as much. In the absence of AMS the relaxation time of the negative change was 126 ± 4 s, compared to 83.6 ± 3.6 and 84.1 ± 4.2 s in the presence of 0.2 and 0.52 M AMS, respectively. The results are consistent with previous findings that the rate of *cis-trans* proline isomerization in RNase-A is only weakly dependent on AMS concentration (Schmid, 1981; Lin & Brandts, 1983c).

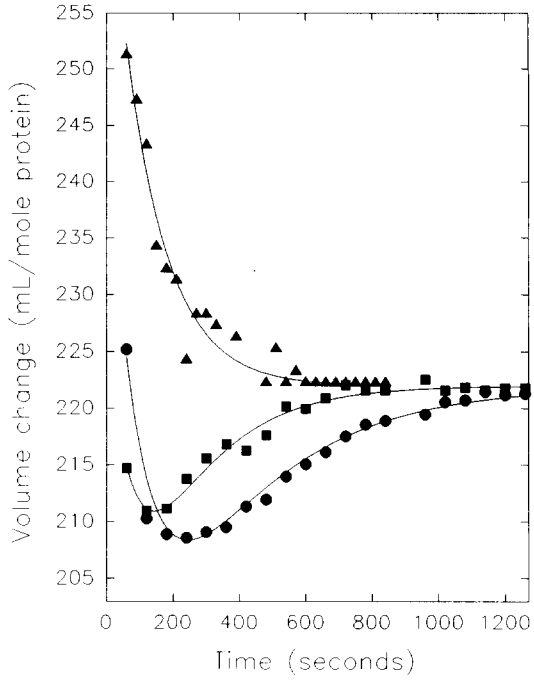

Fig. 2. Time dependence of the slow volume change of RNase-A refolding as a function of $(NH_4)_2SO_4$ concentration. Protein concentrations ranged from 5 to 10 mg/mL. Final conditions were 2.5 M GuHCl, 33 mM histidine, pH 6.5–7, with: (1) 0.0 M $(NH_4)_2SO_4$, curve replotted from Figure 1 (circles—note difference in ordinate scale from Fig. 1); (2) 0.2 M $(NH_4)_2SO_4$ (squares); and (3) 0.52 M $(NH_4)_2SO_4$ (triangles). Curves generated using the fitted values in Table 1 are drawn as solid lines.

Figure 3 presents the individual components comprising the curve shown in Figure 1. The major feature of this deconvolution is the existence of 2 concurrent slow reactions with volume changes of opposite sign. The squares, found by subtracting the curve shown as triangles, obtained in the presence of 0.52 M AMS, from the curve presented as circles, obtained in its absence, trace the positive volume change that is partly hidden by the faster of the 2 slow reactions.

Equilibrium and kinetic CD at 222 and 276 nm

The dichroism at 222 nm is due primarily to secondary structural changes (see, for example, Pflumm et al., 1986, for a study of RNase), whereas changes in the protein's tertiary structure are reflected in the 276-nm signal (reviewed by Sears & Beychok,

Table 1. *Fitted volume changes of RNase-A refolding and the time constants of the slow reactions*[a,b]

[AMS] (M)	ΔV_{fast}	ΔV_1	ΔV_2	ΔV_{net}	τ_1[c]	τ_2[c]
0	+232 ± 13	−63.5 ± 9.8	+53.1 ± 6.7	+222 ± 12	126 ± 4	293 ± 17
0.20	+252 ± 11	−47.9 ± 0.4	+41.7 ± 1.1	+246 ± 11	83.6 ± 3.6	191 ± 12
0.52	+263 ± 2	−49.8 ± 9.3	–	+213 ± 7	84.1 ± 4.2	–

[a] Volume changes are in mL/mol of protein.
[b] Curves are drawn in Figures 1, 2, and 3 using the fitted values.
[c] Time constant, τ, in s, where $\tau = 1/k$; k = rate constant.

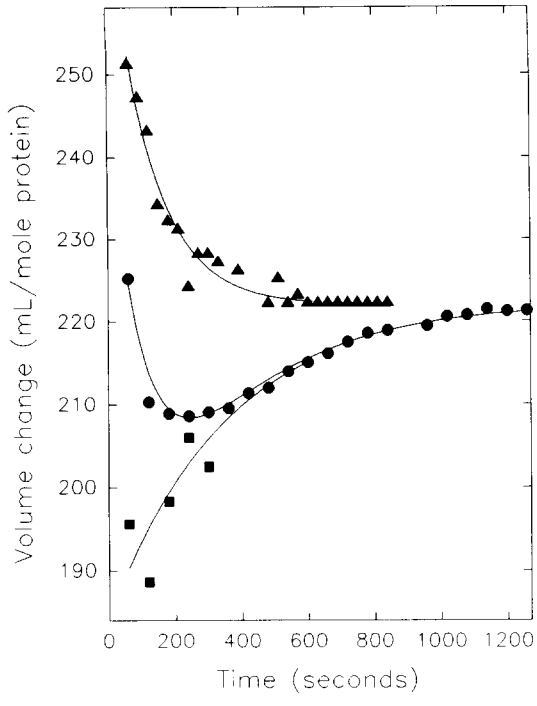

Fig. 3. Deconvoluting the volume change attending the refolding of RNase into 3 components: (1) a volume rise that occurs within the mixing dead time of 1–2 min (note scale on ordinate), (2) a slow negative volume change (triangles), and (3) a very slow positive volume change (squares merging with curve from Fig. 1). Circles, curve from Figure 1 replotted (note difference in ordinate scale from Fig. 1); triangles, volume change of refolding with 0.52 M $(NH_4)_2SO_4$. The squares are obtained by subtracting the curve shown as triangles from the curve given as circles. Solid lines represent the fitted curves calculated as in the text.

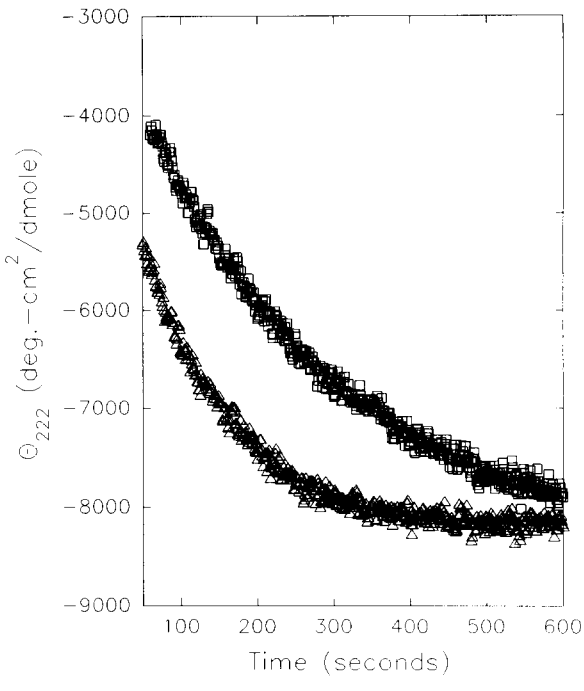

Fig. 4. Kinetic CD at 222 nm of RNase refolded in the absence (squares) and presence (triangles) of 0.52 M $(NH_4)_2SO_4$. The molar ellipticity was calculated on the basis of the mean residue weight.

1973; Kahn, 1979). Backbone rearrangements were therefore monitored by CD at 222 nm, shown in Figure 4, and the effect of AMS on the kinetics of these changes was examined. The CD reached the same equilibrium value with AMS as without it. The curve-fitting results, presented in Table 2, show that the CD signal *change* at 222 nm due to folding in the absence of AMS was −5,999 deg-cm^2/dmol with a time constant of 266 ± 39 s. In the presence of additive, the *change* in CD intensity was −4,697 deg-cm^2/dmol of residues, with a time constant of 119 ± 17 s. The difference due to folding between the parallel experiments with and without AMS was −1,302 deg-cm^2/dmol.

CD changes in the near-UV are shown in Figure 5, the curve-fitting results being presented in Table 2. In the absence of AMS the 276-nm CD folding amplitude was −23,490 deg-cm^2/dmol of protein with a time constant of 248 ± 26 s. This indicates large side-chain rearrangements that affect 1 or more of the 6 tyrosines of the protein (see Discussion) and, possibly, the disulfides (RNase-A contains no tryptophan). In the presence of 0.52 M AMS, the change in 276-nm dichroism was diminished from −23,490 to −19,198 deg-cm^2/dmol at a time constant of 118 ± 4 s.

The parallel kinetic CD experiments in the near- and far-UV demonstrate that the slower of the 2 slow events is rate-limiting and yields first-order kinetics. The faster process, which is also first order, is only uncovered when the slower reaction is moved into the dead time by AMS.

Discussion

This is the first use of volumetric measurements as a probe in protein folding. We therefore begin by fitting the present work into the context of existing models of RNase folding, noting that the data demonstrate 2 concurrent slow events. To reinforce this discussion, the correlation between the volumetric and CD data is examined next, as it establishes that the former arises from structural changes in the protein. Because the CD spectrum of RNase has been well studied both experimentally and theoretically, which is unusual, one is able to make inferences as to the molecular bases of the structural changes. We then discuss the 3 kinetic events that we detect: the fast step, which is completed in the mixing dead time, and each of the 2 slow events. In the course of this part of the discussion we relate the work to current RNase folding models in more detail. We examine the role of water of hydration, particularly in the fast step, where we estimate the number of water molecules expelled from the protein surface. The formation of packing defects within the protein is also considered. Finally, we relate both the work presented here and present models of RNase folding to the broader question of folding in general.

Volume change demonstrates two concurrent slow-folding events

The slow-folding kinetics were first order when followed by tyrosine absorbance at 287 nm (data not shown), in accord with previous findings (Kim & Baldwin, 1980; Lin & Brandts, 1983c). It has been argued that the folding kinetics under these conditions are due primarily to *cis–trans* isomerization of proline 93 (Kim & Baldwin, 1980; Schmid, 1983). However, the results pre-

Table 2. *Fitted refolding parameters from CD at 222 and 276 nm in the absence and presence of 0.52 M AMS*[a]

$\Delta[\Theta]_{222}$[b]	$\Delta[\Theta]_{222,AMS}$	$\Delta\Delta[\Theta]_{222}$	τ_{222}[c] − AMS	τ_{222} + AMS
−5,999 ± 626	−4,697 ± 589	−1,302 ± 860	266 ± 39	119 ± 17
$\Delta[\Theta]_{276}$[b]	$\Delta[\Theta]_{276,AMS}$	$\Delta\Delta[\Theta]_{276}$	τ_{276}[c] − AMS	τ_{276} + AMS
−23,490 ± 328	−19,198 ± 1,135	−4,293 ± 1,181	248 ± 26	118 ± 4

[a] AMS designates experiments done in 0.52 M $(NH_4)_2SO_4$.
[b] Ellipticities at 222 nm are based on mean residue weight. Ellipticities at 276 nm are based on the whole protein molecular weight. Units are deg-cm^2/dmol.
[c] Time constants, τ, in s, where $\tau = 1/k$; k = rate constant.

sented in Figures 1, 2, and 3, the deconvolution of 2 first-order processes from them, and the opposite signs of the corresponding volume changes demonstrate that the first-order kinetic phase observed by absorbance is actually composed of 2 concurrent slow reactions. The volumetric properties of the 2 slow reactions allow them to be distinguished from one another, which is not possible by absorbance (Brandts et al., 1975). Insofar as these processes may arise from different forms in a heterogeneous mixture of denatured forms, we begin to observe different refolding pathways. Alternatively, the 2 reactions may occur in the same molecule, which would, in that case, exhibit parallel and independent refolding of its parts.

The AMS sensitivity of the volume change helps to identify the molecular origin of the 2 slow events. In moderate concentrations of AMS there is a significant decrease in amplitude and time constant of the slow positive change and a concomitant increase in amplitude of the fast volume change. The slow positive volume change is thus accelerated, displacing its amplitude into the dead time of mixing. In contrast, the rate of the negative volume change is increased by a smaller amount upon addition of 0.2 M AMS and unchanged by further AMS up to 0.52 M.

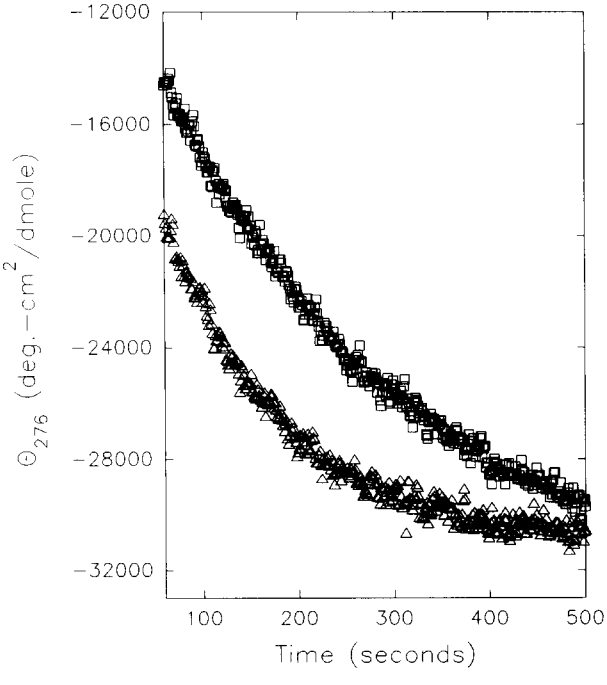

Fig. 5. Kinetic CD at 276 nm of RNase refolded in the absence (squares) and presence (triangles) of 0.52 M $(NH_4)_2SO_4$. The molar ellipticity was calculated on the basis of whole protein.

Previous studies have demonstrated that *cis-trans* isomerization of proline 93 is only weakly dependent on AMS concentration (Schmid, 1981; Lin & Brandts, 1983c). The slow negative volume change observed in the present study shows this behavior, which suggests that it may arise from structural changes during the course of proline isomerization. On the basis of its rate, which is typical of isomerization about proline peptide bonds (Kim & Baldwin, 1980; Lin & Brandts, 1983c; Schmid, 1983; see also discussion below), and weak sensitivity to the AMS concentration, we assign the reaction attended by a negative volume change to proline isomerization.

The slow event attended by a volume change of +53 mL/mol of protein does not have properties of proline isomerization. Firstly, its time constant (Table 1) is much larger than that of proline isomerization, which is typically well below 200 s, depending on the concentration of denaturant and pH (Lin & Brandts, 1983c). Secondly, the reaction is strongly dependent on AMS in both the volume change and CD experiments. These findings are consistent with the work of Lin and Brandts, who observed a single first-order reaction with a time constant of 300 s when the protein was refolded in the absence of AMS. They found that adding 0.52 M AMS accelerated the reaction and separated the first-order curve into a slow event (τ = 130 s) and a fast reaction (τ = 17 s) (Lin & Brandts, 1983c), the second of which we would not see with a 1-2-min mixing dead time.

The complex kinetics of Figure 1 could be explained by supposing that the rate of proline isomerization is not constant but is slowed by the formation of intermediate structures. However, refolding was carried out under conditions where folding intermediates are unstable (Kim & Baldwin, 1980; Schmid, 1983). Moreover, recent findings suggest that the formation of intermediate structure would enhance, not slow down, proline isomerization (Texter et al., 1992). Although there is reasonable evidence that AMS has no direct effect on the isomerization of prolyl peptide bonds (Schmid, 1981; Lin & Brandts, 1983c), it is known to stabilize structure (von Hippel & Wong, 1965) and is often used to induce the formation of folding intermediates in RNase-A (Kim & Baldwin, 1980; Udgoankar & Baldwin, 1988). In turn, the formation of intermediates may increase the

rate of proline isomerization (Schmid & Baldwin, 1978; Cook et al., 1979; Schmid & Blaschek, 1981; Schmid, 1986). Texter et al. (1992) recently showed, in addition, that the replacement of residues that hydrogen bond with a proline in dihydrofolate reductase alters the rate of *cis–trans* isomerization. However, *cis–trans* prolyl isomerase, which catalyzes proline isomerization (Fischer et al., 1984; Fischer & Bang, 1985; Evans et al., 1987; Lang et al., 1987), apparently does not enhance the rate of the AMS-sensitive step in the refolding of RNase-A (Lin & Brandts, 1984).

The reaction accompanied by a positive volume change and which is highly sensitive to AMS has kinetic properties of the "XY" process proposed by Lin and Brandts to dominate the slow kinetics of RNase-A refolding (Lin & Brandts, 1983c, 1984, 1987, 1988). These similarities suggest that the slow positive volume change arises from structural changes resulting directly from the Y-to-X interconversion. Detectable until now only by its absorbance and fluorescence kinetics, the transition is between forms of unknown conformation; hence the designations Y and X for its initial and final states.

The problem of determining which prolines in RNase-A are responsible for slow folding was examined recently by making single and double mutations (Schultz & Baldwin, 1992). These workers concluded that both prolines 93 and 114 contribute to the slow-folding species, which they designated U_S. The folding rate of the double mutant was dependent on GuHCl concentration, going from 10 to 100 s over the experimental range of denaturant concentrations (Schultz et al., 1992). They suggested that the GuHCl-sensitive kinetics were due to the refolding of the fast folding species, U_F. However, it is also plausible to suggest that the slow kinetics observed in the refolding of the double mutant are due to the Y-to-X reaction because this event, in addition to being strongly sensitive to AMS, is also markedly slowed by denaturant (Lin & Brandts, 1983c). On balance, it appears that proline isomerization is probably not the dominant contributor to the AMS-sensitive event.

Slow volume changes are the result of structural changes

The slow positive volume change (ΔV_2) involves changes in the secondary structure because the time constant of CD experiments at 222 nm in the absence of AMS agrees well with the time constant obtained from volumetric data: 266 ± 39 and 293 ± 17 s, respectively. The difference is not statistically significant (Student's *t*-test, $P > 0.30$). The time constants of ΔV_2 and the CD experiments at 276 nm also agree reasonably well (compare results from Tables 1 and 2; $P > 0.1$), indicating that ΔV_2 also includes changes in tertiary structure.

In 2 M urea, 0.56 M AMS, 0.05–0.1 M acetate buffer, pH 5.2, 10 °C, the time constant of proline isomerization as measured by absorbance is 130 s (Lin & Brandts, 1983c), which is close to our CD results of 118–119 s (Table 2), given our slightly different refolding conditions (2.5 M GuHCl, 0.52 AMS, 0.033 M histidine, pH 6.5, 20.0 °C for dilatometry and 21–23 °C for CD). The agreement supports our assignment that the negative volume change is proline isomerization. In 0.52 M AMS, the time constant of the negative volume change was 84 ± 4 s, which is somewhat faster than the 119 ± 17 s of the corresponding CD experiment at 222 nm, suggesting that in the presence of AMS, the 2 techniques see somewhat different aspects of the process.

In the absence of AMS at 222 nm, the time constant was 266 ± 39 s. The corresponding time constant at 276 nm was 248 ± 26 s. The close agreement between time constants at the 2 wavelengths implies that changes in 3-dimensional structure are the concerted result of secondary and tertiary rearrangements. The same is true when AMS is present: $\tau = 119 \pm 17$ s at 222 nm and 118 ± 4 s at 276 nm. These results are inconsistent with previous suggestions that proline isomerization does not cause structural changes other than the isomerization itself (Lin & Brandts, 1983c). Although the native crystal structure of RNase-A can be fitted with either *cis* or *trans* proline 93 (Wyckoff et al., 1970), this observation does not exclude the possibility that substantial structural changes can occur as a consequence of *cis–trans* proline isomerization *during folding*.

Possible sources of CD at 222 and 276 nm

The CD signal at 222 nm in proteins arises predominantly from the peptide bonds (Yang et al., 1986). However, a fraction of the signal can also arise from aromatic side chains (Strickland, 1972). Just as the n–π^- transition of the peptide bond peaks at 225 nm (Donovan, 1969), so does the ^1L_a transition of the tyrosyl ring (Goux & Hooker, 1975). In the absence of AMS, the change in ellipticity observed on folding was −5,999 ± 626 deg-cm^2/dmol. Although some of this change in signal is undoubtedly from the tyrosyl transition (there are 6 tyrosine residues in RNase-A and no tryptophan), the strong negative band at 222 nm in the native form must arise primarily from the peptide transition because the ^1L_a at this wavelength is positive (Goux & Hooker, 1975). The tyrosines would thus contribute a rise in ellipticity on folding, when a decrease is what is seen. In the presence of AMS the change in far-UV dichroism, −4,697 ± 589 deg-cm^2/dmol, is still substantial (Table 2). These results indicate that both slow reactions involve backbone rearrangements.

In large part, the near-UV CD signal observed in native RNase-A arises from interactions among the 6 tyrosyl side chains within the protein. There are 3 tyrosine pairs that contribute significantly: tyrosines 92 and 97, tyrosines 25 and 97, and tyrosines 73 and 115. These couplings produce about 40% of the CD intensity at 275 nm (Strickland, 1974), most of the rest arising from the disulfides (Horwitz et al., 1970, and see below). Because 1 tyrosine pair contributes more to the native CD signal than the others, it is possible to suggest areas of the molecule that undergo slow conformational changes. The interaction of tyrosines 73 and 115 is by far the strongest, contributing about −12,210 deg-cm^2/dmol at 276 nm, whereas the interactions of tyrosines 25 and 97 and tyrosines 92 and 97 are both significantly weaker (Strickland, 1972). The changes in the near-UV CD signal observed here on folding in the presence of AMS, amounting to −19,198 deg-cm^2/dmol, are probably due, in part, to changes that affect the geometry of tyrosines 73 and 115. This pair is far from proline 93, so that any structural changes caused by the proline would have to be transmitted through the molecule. It is also possible that the CD signal is brought about by effects of proline 114 isomerization on tyrosines 73 and 115. This proline, which is very close to both tyrosine residues, has been shown recently to isomerize to a significant extent (Adler & Scheraga, 1990). Effects of the 2 isomerizing prolines, of course, are not mutually exclusive.

Although rotation about disulfide bonds, of which RNase has 4, has been proposed as a rate-limiting step in folding (Kessler

& Rundel, 1968; Fraser et al., 1971; Mui et al., 1985), this is unlikely in view of rapid rotational equilibration about the disulfide of cystine in solution (Kahn & Beychok, 1968). Whatever their exact source, the substantial changes in the near-UV CD require tertiary rearrangements during the slow phases, changes that appear to be concerted with secondary structural alterations.

Early formation of compact structure and deprotonation due to pH jump

Most current folding models are based on a hierarchical formation of structure (for reviews, see Kim & Baldwin, 1990; Ptitsyn et al., 1990; Jaenicke, 1991; Matthews, 1991). Relatively compact structures are believed to form in the early stages of folding (Kuwajima, 1989; Matthews, 1991; see also below). This is observed in the volume change data as a large amplitude change that occurs within the mixing dead time of the experiments. ΔV_{fast}, however, is a sum of volume change contributions arising from (1) the rapid formation of local compact structures and (2) deprotonation of the protein due to the pH jump required to initiate refolding. The contribution of (1) can be extracted from ΔV_{fast} if the magnitude of (2) is known. The magnitude of (2) can be estimated by finding the total number of protons removed from each type of titrating group as a result of the pH jump and then multiplying by the volume change of deprotonating that kind of group. The numbers of protons removed can be estimated by using the pK_a values of simple amino acids to describe the denatured state at pH 2, obtaining the number of bound protons at this pH. The native state at pH 6.5–7 is described by the pHs of half titration, $pK_{1/2}$, as found in electrostatic calculations (Matthew & Richards, 1982). It is important to use $pK_{1/2}$ values because charge interactions between nearby side chains can significantly alter the pK_a values of the titrating groups (Tanford & Kirkwood, 1957; Matthew & Richards, 1982). The differences between the 2 sets of calculations yield the total number of protons removed from each titrating group. The pH jump from 2 to 6.5–7 will deprotonate—either wholly or in part—the carboxyls, side-chain imidazoles, and the N-terminal amino group. Deprotonating carboxyl groups in proteins gives a volume change of approximately +11 mL/mol H^+ removed when the transfer of the proton to hydroxide is taken into account, whereas a side chain imidazole and N-terminal amino group each yields a change of +23 mL/mol (Kauzmann et al., 1962; Rasper & Kauzmann, 1962; see also Ybe, 1991 and references therein). RNase contains 11 carboxyls: 5 Asp, 5 Glu, and the carboxy-terminus, all of which will titrate in this pH range, yielding +121 mL/mol protein. There are 4 histidines of which we estimate that 1.9 titrate, as does the α-amino-terminus. At +23 mL/mol H^+, this comes to +66.7 mL/mol protein, making the overall volume change of deprotonation +121 + 66.7 = 188 mL/mol RNase. Therefore, from the total fast volume change of +232 mL/mol of protein in the absence of AMS subtraction of 188 mL/mol of protein for deprotonation yields +44 mL/mol of protein as the contribution to the fast volume change of refolding of all processes other than proton titration, in this case, the formation of compact structure. We estimate the error in this figure to be ±17 mL/mol. The +44-mL/mol amounts to 0.5% of the native protein's partial molar volume of 9,619 mL/mol (Ulrich et al., 1964).

Fast-folding species constitute approximately 20% of the denatured population under the solution conditions of Garel and Baldwin (1973), Garel et al. (1976), and Lin and Brandts (1983c). We estimate that under the present experimental conditions, which are similar but not identical, they represent 13% (Ybe, 1991). The volume change of the fast-folding species can therefore be estimated. Pressure-induced unfolding of small proteins typically yields ΔVs ranging from −50 to −100 mL/mol of protein (Zipp & Kauzmann, 1973), which would, of course, be positive in sign in the folding direction. Taking 13% of this range yields an upper limit of +7 to +13 mL/mol of protein for the volume change expected to arise from the refolding of the fast-folding species. However, this upper limit is significantly smaller than that part of the fast volume change attributable to folding, +44 mL/mol of protein. Therefore, the measured fast volume change of refolding must, for the most part, arise from the rapid formation of compact structures in species which must undergo further slow isomerizations to become native.

When a random polypeptide chain folds into its native 3-dimensional structure, apolar side chains are transferred into the interior of the protein. Consequently, water of hydration is expelled into the bulk solvent (for reviews, see Kauzmann, 1959; Desnoyers, 1977). Normally the density of that water drops, and a positive volume change is observed. The water expelled in the course of early hydrophobic collapse thus appears to be responsible for most of the +44-mL/mol change in volume. This corresponds to 73 $Å^3$ per molecule of protein. The molar volume of water, 18 mL/mol, corresponds to 30 $Å^3$ per molecule of solvent. If the water of hydration were to change in density by as much as 1%, or 0.3 $Å^3$ per molecule upon expulsion into the bulk, the number of water molecules expelled would be 73/0.3 = 240, a figure that could be an underestimate because the density difference averaged over the denatured protein's surface may well be less than 1%. The value can be compared with the approximately 60 waters expelled from hemoglobin in the course of the R to T switch (Colombo et al., 1992). The expulsion of these water molecules during folding will make a substantial favorable contribution to the entropy of the process.

The slow volume decrease: Volumetric consequences of proline isomerization

If the assignments made above are correct, the volume change of the folding process whose kinetics are controlled by proline isomerization in RNase-A is −64 mL/mol of protein. This is the first time the volume change resulting from a proline reaction has been measured. Caution is advised, however, in attributing it to *cis-trans* isomerization about the proline peptide bond per se. There is no reason to believe such isomerization would produce a significant volume change in and of itself. It is much more likely that events occurring elsewhere in the protein but whose kinetics are rate limited by proline isomerization are responsible.

Were the volume change to arise from the expulsion of water of hydration, one would expect an increase in volume as described above. The observed decrease may come from a tighter packing of atoms both near the prolines undergoing change and elsewhere in the molecule. If this is the case, hydration changes in this step of the folding, if any, are small relative to the reduction in volume due to improved packing of atoms in the interior of the protein. The isomerization of proline 93 may also contribute to the observed negative volume change by withdraw-

ing tyrosine 92 from the solvent as the proline goes from *trans* to *cis*. Model compound studies have shown that the transfer of aromatic residues from an aqueous to nonpolar environment entails a negative volume change (Kasarda, 1970; Weber et al., 1974; Li et al., 1976).

The slow volume increase: Formation of packing defects

The slow positive volume change of +53 mL/mol of protein may arise from the expulsion of water of hydration and its attendant fall in density or it may be due to an increase in the overall volume of packing defects within the protein, or both. To assess the role of packing defects, we estimated the volume increase of creating the void spaces known to be present in the interior of the protein. The volumes of the cavities were found by taking the dimensions of each cavity in RNase-S from Lee and Richards (1971). RNase-S is essentially identical in structure to RNase-A (Richards & Wyckoff, 1971). Cavity A is formed by valines 54, 57, and 108, and isoleucine 106. Cavity B is larger and is bounded by phenylalanines 8 and 120, valines 47, 54, and 108, and isoleucine 106, whereas the smallest cavity, C, is bounded by valines 54, 108, and cysteine 58. It is worth noting that the cavity volume reported by these workers is that volume of space which can be occupied by the *center* of the probe, which is a water molecule represented as a sphere of radius 1.4 Å. By definition, a space large enough to fit 1 water molecule, but not large enough for it to move around inside, has a volume of 0.

Lee and Richards (1971) determined the volume of cavity A to be 0.029 $Å^3$, which is equivalent to the volume of a sphere of radius 0.191 Å. We calculated the volume of the cavity by adding the radius of a water molecule (1.4 Å) to 0.191 Å, and then determining the volume of the new equivalent sphere of radius 1.59 Å. This method yields cavity volumes of 16.87 $Å^3$, 26.52 $Å^3$, and 12.51 $Å^3$ for cavities A, B, and C, respectively, a total void space due to these cavities of 55.9 $Å^3$/molecule, or a volume increase of +33.7 mL/mol relative to a compact intermediate state lacking the 3 cavities. Considering the roughness of the cavity volume estimate, this is in reasonable agreement with the experimentally measured change of +53 mL/mol of protein. Therefore, we suggest that the slow positive volume change arises primarily from rearrangements which form packing defects in the interior of the protein during the late stages of refolding. This does not exclude a small additional positive contribution from expulsion of water of hydration from parts of the molecular surface.

Comments on existing folding models of RNase-A

There are currently 3 models that attempt to describe the folding of small monomeric proteins. (1) The framework model asserts that an intermediate with approximately native secondary structure is formed before the tertiary structure is locked into place (Kim & Baldwin, 1982). The molten globule structure adds to this the concept that the resulting intermediate is compact and has a fluctuating tertiary structure (Ptitsyn, 1987; Kuwajima, 1989; Ptitsyn et al., 1990). (2) The subdomain model submits that the protein folds in parts, and different subdomains coalesce later (Oas & Kim, 1988; Staley & Kim, 1990). (3) The simple kinetic model proposed for the folding of RNase-A is based on a 2-state transition between the native and an ensemble of unfolded forms (Lin & Brandts, 1983d). It offers that rapid steps in the folding follow the slow reactions and that the different slow reactions arise from different populations of denatured forms.

In support of the framework model, at least 2 folding intermediates have been discovered (Cook et al., 1979; Kim & Baldwin, 1980). The rate-limiting step is thought to involve the *trans–cis* isomerization of proline 93 (Cook et al., 1979). However, the last aspect of this model is inconsistent with the volume change and CD results that there are 2 slow concurrent reactions. The presence of 2 concurrent slow reactions is consistent with the simple model of Lin and Brandts (1983d). However, this model fails to explain why the early formation of compact structures is detected in the volume change experiments. The model explicitly states that fast reactions can only occur after the slow reactions. The data presented here are thus compatible with elements of both of these models.

The need to combine features of both models suggests that RNase-A may be able to access multiple folding pathways. A calculation of how long it would take a small protein to search through all possible conformations for the native structure convinced many that protein folding proceeded along a well-defined pathway (Levinthal, 1969). However, Harrison and Durbin (1985) correctly pointed out that the length of a random search could be drastically reduced to a biologically relevant time scale by simply keeping those transient structures that are native-like. This was supported by recent theoretical calculations (Zwanzig et al., 1992). Moreover, they argued that it is possible for the protein to proceed via a jigsaw-puzzle pathway, i.e., a folding mechanism that has many parallel folding channels. Indeed, if the denatured population is a heterogeneous mixture of different denatured states, it is plausible to argue that many folding channels are taken to the native structure. This appears to be the case in the folding of dihydrofolate reductase (Kuwajima et al., 1991), *trp* aporepressor from *Escherichia coli* (Gittelman & Matthews, 1990), and recombinant human macrophage colony-stimulating factor (Wilkins et al., 1993).

The folding mechanism of RNase-A has been under study for many years. Most workers believe that intermediates are formed along a sequential pathway, in support of the framework model (Kim & Baldwin, 1982), and that there is a single slow step (Cook et al., 1979; Schmid, 1983, 1986). However, experimental work presented here and in the past indicates that the nature of the folding kinetics ultimately depends on the folding conditions adopted, an observation consistent with emerging evidence that proteins can adopt a number of folding pathways (Leopold et al., 1992, and citations above). It is shown here that under conditions which destabilize intermediates, 2 concurrent slow events are present, as detected by volume change and CD. These data will have to be accommodated by any model or set of models of RNase refolding. The volumetric results, in particular, being of a macroscopic thermodynamic property, must be satisfied by any mechanism based on nonmacroscopic procedures.

Materials and methods

Crystalline bovine pancreatic RNase-A (R-5500) was purchased from Sigma Chemical Company and used without further purification. Ultraviolet grade GuHCl, obtained from United States Biochemicals, was routinely dried over P_2O_5 in vacuo for

at least 1 week before use. All other chemicals used were of reagent grade. The building's distilled water was further purified by passage through a Barnstead unit containing charcoal, demineralizing, and submicron filters. Its conductivity did not exceed 10^{-6} ohm^{-1}.

Denatured protein solutions used in the volume change and CD work were made up in a pH 2 buffer (40 mM histidine) containing 3 M GuHCl and, at times, AMS (0.24–0.52 M). They were dialyzed at 4 °C and filtered before use through 0.45-μ disposable nylon filters.

Protein concentration was determined by absorption using the extinction coefficient of native RNase-A, 0.71 mL/(mg-cm) at 278 nm (Sela & Anfinsen, 1957). Spectra were obtained at room temperature using a Cary 17D recording spectrophotometer.

The amount of acid or base needed to lower or raise the pH of protein solutions was determined by titrating a 5-mL aliquot with 6 M HCl or 1 M NaOH. The pHs were measured on a Radiometer PHM64 instrument with a GK231C combined electrode for semi-micro samples and a GK2401C electrode for all other solutions. The pH meter was calibrated routinely at room temperature with standard pH 4 and pH 7 buffers obtained from Fisher Scientific. Asymmetry potentials of the electrodes were never less than 90%.

Volume change measurements

Volume changes were measured in modified Carlsberg dilatometers (Katz, 1972; Kupke, 1973; Kahn et al., in prep.). Refolding was carried out in varying amounts of AMS. High protein concentrations (5–21 mg/mL) were necessary to get good separation between protein and buffer signals. In a typical experiment 15 mL of protein solution containing 0–0.52 M AMS were loaded into 1 leg of a large dilatometer using a syringe microburette (Micrometric Instrument Company, Tampa, Florida). The other leg was filled with 3 mL of base of sufficient concentration to yield the desired final conditions (2.5 M GuHCl, 0–0.52 M AMS, 33 mM histidine, pH 6.5) after mixing the contents of the legs. The rest of the dilatometer was filled with HPLC-grade heptane, which acts as manometric fluid.

The units were then chilled briefly in ice so that upon later thermal equilibration at 20.0 ± 0.001 °C, expansion of the heptane ensured that the unit was completely filled with the manometric fluid and without gas bubbles. Once the unit was cool, a calibrated capillary was put into place, sealing the apparatus, and the assembled unit was transferred to the 20.0 °C constant temperature bath. Before starting the experiment, the heptane level was adjusted to a convenient height. A baseline heptane level in the capillary was established by readings at 1-min intervals for a minimum of 10 min.

After establishing the baseline, the contents of the legs were mixed by tipping the unit from side to side 15 times. Readings of the heptane height were continued at 1-min or 30-s intervals until there was no further change in the level. The difference between the initial baseline and the new heptane height at any time yielded the volume change. The mixing dead times were typically 1–2 min.

Heptane, the manometric fluid, has a large coefficient of thermal expansion, so that a small fluctuation in bath temperature will result in an artifactual volume change. Control experiments were therefore necessary to ensure that the slow changes did not arise from this source. A dilatometer containing plain water and heptane equal in volumes to those in protein-containing experiments was placed in the tank with units containing protein. The heptane level in the temperature control unit remained unchanged throughout the experiments, and no slow changes were observed in the dilution and buffer titration controls (see below). To avoid slow volume changes from incomplete mixing, protein concentrations were kept below 1.6 mM (22 mg/mL), and the dilatometers were throughly mixed by tipping from side to side 15 times, as mentioned above. The mixed solutions were checked for homogeneity by remixing after the heptane level stabilized. A second mix volume change, which is indicative of incomplete mixing, was not observed.

The overall volume change experiment includes (1) the volume change of refolding and titrating the protein, (2) the volume change of diluting the protein, and (3) the volume changes of diluting the guanidine-containing buffer and of titrating the buffer with base. The combined volume change of refolding and titrating the protein, (1), is found by subtracting the contributions of (2) and (3) from the volume change of the overall experiment. The volume change of diluting the protein was determined by loading 1 leg of a dilatometer with 15 mL of denatured protein solution and loading the other leg with 3 mL of pH 2 dialysis buffer with which the unfolded protein had been in equilibrium. These volume changes were negligible. The volume change of diluting and titrating the buffer was measured in each experiment by loading 1 leg of the dilatometer with 15 mL of pH 2 dialysis buffer, with which the protein had been in equilibrium, and the other leg with 3 mL of NaOH solution of sufficient concentration to obtain the desired final pH. These controls were run at the same time as the protein refolding experiments.

In experiments at high AMS concentrations the top of the heptane column separated into short pieces in the course of mixing the solutions in the dilatometer. The raw initial volume changes in this case were large, negative, and rapid on the hand-mixing time scale. Some heptane was thus left on the inner walls of the capillary as the meniscus fell. As this heptane ran down toward the meniscus, it formed short droplets, trapping air beneath them. These remained stable relative to one another, changing in position within the capillary en bloc as the overall heptane level changed with time. The kinetics were unaffected, as the separation of the heptane column was over within the dead time of mixing. To obtain correct equilibrium volume changes we modified the tops of the capillaries, widening them into conical bowls. Once the heptane level had stabilized, the dilatometer was warmed while still in the constant temperature bath by gently grasping 1 leg with the hand. This caused the heptane level to rise to the top of the capillary, expelling the trapped air. As soon as the air was expelled, which took 3–5 s, the hand was withdrawn, and the now rejoined heptane column was allowed to fall to its equilibrium value. Readings were then taken every 10 min for 1 h. The units were mixed again and several readings were made thereafter to ensure constancy of the level.

Two capillaries were used. They were calibrated individually by filling their working lengths with mercury, measuring the temperature of the room and the length of the mercury column, and expelling and weighing the mercury. Standard tables of the density of mercury against temperature then yielded the capillary calibration (Kahn & Briehl, 1982). The capillaries measured 0.489 and 0.465 μL/cm change in heptane level.

Kinetic CD

The Aviv model 62DS was set up in the kinetic mode and the wavelength fixed at either 222 or 276 nm. Cylindrical cells, purchased from Precision Cells, of pathlengths ranging from 0.5 mm to 1 cm were used. In a typical run, 5 mL of denatured protein solution were added to 1 mL of base in a small test tube, mixed, taken up into a syringe, and quickly filtered directly into the CD cell. The mixing dead time was measured and found to be 40–60 s. Data were collected until there was no further change in ellipticity. Two kinetic runs were baseline corrected and then averaged before being fitted to obtain time constants and amplitudes of exponential decays. Ellipticities are in units of deg-cm^2/dmol. Data at 222 nm were expressed on the basis of mean residue weight, whereas those in the near UV are on a whole protein basis.

Analysis of volumetric data

The volume change of refolding was modeled as the sum of ΔV_{fast} and 2 exponentials, one representing the slow negative volume change and the other representing the slow positive change. In the absence of AMS, the net volume change at time t, $\Delta V(t)_{net}$, is described by:

$$\Delta V(t)_{net} = \Delta V_1 \exp(-k_1 t) - \Delta V_2 \exp(-k_2 t) + \Delta V_3, \quad (1)$$

where ΔV_1 and ΔV_2 are the amplitudes of the slow negative and positive volume changes, respectively, k_1 and k_2 are the rate constants, and ΔV_3 is the net equilibrium volume change. Bearing in mind that ΔV_1 is negative whereas ΔV_2 is positive, the fast volume change, ΔV_{fast}, was obtained by subtracting ΔV_1 and ΔV_2 from $\Delta V(0)_{net}$.

In the presence of 0.35–0.52 M AMS, the slow positive change (ΔV_2) is displaced into the mixing dead time, and Equation 1 reduces to:

$$\Delta V(t)_{net} = \Delta V_1 \exp(-k_1 t) + \Delta V_{3AMS}, \quad (2)$$

in which ΔV_1 is the amplitude of the slow negative change, k_1 is its rate constant, and ΔV_{3AMS} is the net equilibrium volume change in the presence of AMS. ΔV_{fast} in this case was obtained by subtracting ΔV_1 from ΔV_{3AMS}.

The amplitudes and rate constants of the 2 slow reactions at various concentrations of AMS were obtained by fitting Equation 1 to the experimental data using the commercial nonlinear regression package, NFIT 1.0 (Island Products, University of Texas Medical Branch, Galveston, Texas). The amplitude and rate constant of the negative volume change used as initial input to the regression for the first term in Equation 1 were found by using the values obtained by fitting Equation 2 to one of the 0.52 M AMS experiments. Initial estimates of the amplitude and rate constant of the slow positive volume change were obtained by fitting a single exponential to the data at times greater than 300 s. Equation 1 was then fitted to each of the 3 experiments done in the absence or at intermediate concentrations of AMS. The resulting constants were averaged, the means and standard deviations being shown in Table 1. Equation 1 was also fitted to a single data set made up by averaging all experiments performed in the absence of AMS to obtain the curve in Figure 1.

Analysis of CD kinetics

To obtain time constants and amplitude changes, the kinetic CD scans were fitted to the expression:

$$[\theta(t)] = A \exp(-kt) + [\theta]_e, \quad (3)$$

where $[\theta(t)]$ is the molar ellipticity at 222 or 276 nm at time t, $[\theta]_e$ is the molar ellipticity at equilibrium, A is the amplitude of the slow change, and k is the rate constant. Initial estimates of rate constants and amplitudes were obtained from standard semilog analysis. The estimates were then used for nonlinear least-squares fitting as above.

Acknowledgments

We thank Dr. Peter Lipke for a critical reading of the manuscript. The steady encouragement of Dr. Herbert Schoen was greatly appreciated. We are pleased to acknowledge support of the Center for Advanced Food Technology (CAFT) of Rutgers University and of the New Jersey Agricultural Experiment Station (papers D-01405-93-3 and D-10535-93-5). CAFT is a New Jersey Commission on Science and Technology center.

References

Adler M, Scheraga HA. 1990. Nonnative isomers of proline-93 and -114 predominate in heat-unfolded ribonuclease A. *Biochemistry 29*:8211–8216.

Baldwin RL. 1993. Pulsed H/D exchange studies of folding intermediates. *Curr Opin Struct Biol 3*:84–91.

Brandts JF, Halvorson HR, Brennan M. 1975. Consideration of the possibility that the slow step in protein denaturation reactions is due to *cis-trans* isomerism of proline residues. *Biochemistry 14*:4953–4963.

Bycroft M, Matouschek A, Kellis JT Jr, Serrano L, Fersht AR. 1990. Detection and characterization of a folding intermediate in barnase by NMR. *Nature 346*:488–490.

Colombo MF, Rau DC, Parsegian VA. 1992. Protein solvation in allosteric regulation: A water effect on hemoglobin. *Science 256*:655–659.

Cook KH, Schmid FX, Baldwin RL. 1979. Role of proline isomerization in folding of ribonuclease-A at low temperatures. *Proc Natl Acad Sci USA 76*:6157–6161.

Cooke R, Kuntz ID. 1974. The properties of water in biological systems. *Annu Rev Biophys Bioeng 3*:95–126.

Desnoyers JE. 1977. Ionic solute hydration. *Phys Chem Liq 7*:63–106.

Donovan JW. 1969. Ultraviolet absorption. In: Leach SJ, ed. *Physical principles and techniques of protein chemistry, part A*. New York: Academic Press. pp 101–170.

Evans PA, Dobson CM, Kautz RA, Hatfull G, Fox RO. 1987. Proline isomerism in staphylococcal nuclease characterized by NMR and site-directed mutagenesis. *Nature 329*:266–268.

Fischer G, Bang H. 1985. The refolding of urea-denatured ribonuclease A is catalyzed by peptidyl-prolyl *cis-trans* isomerase. *Biochim Biophys Acta 828*:39–42.

Fischer G, Bang H, Mech C. 1984. Nachweis einer Enzymkatalyse für die *cis-trans*-Isomerisierung der Peptidbindung in prolinhaltigen Peptiden. *Biomed Biochim Acta 43*:1101–1111.

Fraser RR, Boussard G, Saunders JK, Lambert JB, Mixan CE. 1971. Barriers to rotation about the sulfur-sulfur bond in acyclic disulfides. *J Am Chem Soc 93*:3822–3823.

Garel JR, Baldwin RL. 1973. Both the fast and slow refolding reactions of ribonuclease-A yield native enzyme. *Proc Natl Acad Sci USA 70*:3347–3351.

Garel JR, Nall BT, Baldwin RL. 1976. Guanidine-unfolded state of ribonuclease-A contains both fast- and slow-refolding species. *Proc Natl Acad Sci USA 73*:1853–1857.

Gittelman MS, Matthews CR. 1990. Folding and stability of trp-aporepressor from *Escherichia coli*. *Biochemistry 29*:7011–7020.

Goux WJ, Hooker TM. 1975. Contribution of tyrosine residues to the optical activity of ribonuclease S. *J Am Chem Soc 97*:1605–1606.

Harrison SC, Durbin R. 1985. Is there a single pathway for the folding of a polypeptide chain? *Proc Natl Acad Sci USA 82*:4028–4030.

Horwitz J, Strickland EH, Billups C. 1970. Analysis of the vibrational structure in the near-ultraviolet circular dichroism spectra of tyrosine derivatives and ribonuclease-A. *J Am Chem Soc 92*:2119–2129.

Jaenicke R. 1991. Protein folding: Local structures, domains, subunits, and assemblies. *Biochemistry 30*:3147–3161.
Kahn PC, Beychok S. 1968. Far-ultraviolet optical activity of crystals in mulls. I. Cystine. *J Am Chem Soc 90*:4168–4170.
Kahn PC. 1979. The interpretation of near-ultraviolet circular dichroism. *Methods Enzymol 61*:339–377.
Kahn PC, Briehl RW. 1982. The absence of volume change in the gelation of hemoglobin-S. *J Biol Chem 257*:12209–12213.
Kasarda DD. 1970. Dilution volume changes of some purine and pyrimidine complexes. *Biochim Biophys Acta 217*:535–538.
Katz S. 1972. Dilatometry. *Methods Enzymol 27*:395–406.
Kauzmann W. 1959. Some factors in the interpretation of protein denaturation. *Adv Protein Chem 14*:1–63.
Kauzmann W, Bodanszky A, Rasper J. 1962. Volume changes in protein reactions. II. Comparison of ionization reactions in proteins and small molecules. *J Am Chem Soc 84*:1777–1788.
Kessler H, Rundel W. 1968. Konformation und gehinderte Rotation in Disulfides und Diseleniden. *Chem Ber 101*:3350–3357.
Kim PS, Baldwin RL. 1980. Structural intermediates trapped during the folding of ribonuclease A by amide proton exchange. *Biochemistry 19*:6124–6129.
Kim PS, Baldwin RL. 1982. Specific intermediates in the folding reactions of small proteins and the mechanism of protein folding. *Annu Rev Biochem 51*:459–489.
Kim PS, Baldwin RL. 1990. Intermediates in the folding reactions of small proteins. *Annu Rev Biochem 59*:631–666.
Kuntz ID Jr, Kauzmann W. 1974. Hydration of proteins and polypeptides. *Annu Rev Protein Chem 28*:239–345.
Kupke DW. 1973. Density and volume change measurements. In: Leach SJ, ed. *Physical principles and techniques of protein chemistry, part C*. New York: Academic Press. pp 1–75.
Kuwajima K. 1989. The molten globule state as a clue for understanding the folding and cooperativity of globular-protein structure. *Proteins Struct Funct Genet 6*:87–103.
Kuwajima K, Garvey EP, Finn BE, Matthews CR, Sugai S. 1991. Transient intermediates in the folding of dihydrofolate reductase as detected by far-ultraviolet circular dichroism spectroscopy. *Biochemistry 30*:7693–7703.
Kuwajima K, Hiraoka Y, Ikeguchi M, Sugai S. 1985. Comparison of the transient folding intermediates in lysozyme and alpha-lactalbumin. *Biochemistry 24*:874–881.
Kuwajima K, Nitta K, Yoneyama M, Sugai S. 1976. Three state denaturation of α-lactalbumin by guanidine hydrochloride. *J Mol Biol 106*:359–373.
Kuwajima K, Sakuraoka A, Fuecki S, Yoneyama M, Sugai S. 1988. Folding of carp parvalbumin studied by equilibrium and kinetic circular dichroism spectra. *Biochemistry 27*:7419–7428.
Kuwajima K, Yamaya H, Miwa S, Sugai S, Nagamura T. 1987. Rapid formation of secondary structure framework in protein folding studied by stopped flow circular dichroism. *FEBS Lett 221*:115–118.
Lang K, Schmid FX, Fischer G. 1987. Catalysis of protein folding by prolyl isomerase. *Nature 329*:268–270.
Lee BK, Richards FM. 1971. The interpretation of protein structures: Estimation of static accessibility. *J Mol Biol 55*:379–400.
Leopold PE, Montal M, Onuchic JN. 1992. Protein folding funnels: A kinetic approach to the sequence-structure relationship. *Proc Natl Acad Sci USA 89*:8721–8725.
Levinthal C. 1969. Are there pathways for protein folding?. In: Debrunner P, Tsibris JCM, Munck E, eds. *Mossbauer spectroscopy in biological systems. Proceedings of the Allerton House meeting*. Monticello: University of Illinois Press. pp 22–24.
Li TM, Hook JW III, Drickamer HG, Weber G. 1976. Effects of pressure upon the fluorescence of the riboflavin binding protein and its flavin mononucleotide complex. *Biochemistry 15*:3205–3211.
Lin LN, Brandts JF. 1983a. Isomerization of proline-93 during the unfolding and refolding of ribonuclease A. *Biochemistry 22*:559–563.
Lin LN, Brandts JF. 1983b. Evidence showing that a proline-specific endopeptidase has an absolute requirement for a *trans* peptide bond immediately preceding the active bond. *Biochemistry 22*:4480–4485.
Lin LN, Brandts JF. 1983c. Mechanism for the unfolding and refolding of ribonuclease A. Kinetic studies utilizing spectroscopic methods. *Biochemistry 22*:563–573.
Lin LN, Brandts JF. 1983d. Mechanism for the unfolding and refolding of ribonuclease A. Simulations using a simple model with no structural intermediates. *Biochemistry 22*:573–580.
Lin LN, Brandts JF. 1984. Involvement of prolines-114 and -117 in the slow refolding phase of ribonuclease A as determined by isomer specific proteolysis. *Biochemistry 23*:5713–5723.
Lin LN, Brandts JF. 1987. Evidence for the existence of three or more slow phases in the refolding of ribonuclease A and some characteristics of the phases. *Biochemistry 26*:3537–3543.
Lin LN, Brandts JF. 1988. Separation of the nativelike intermediate from unfolded forms during refolding of ribonuclease-A. *Biochemistry 27*:9037–9042.
Matthew JB, Richards FM. 1982. Anion binding and pH-dependent electrostatic effects in ribonuclease. *Biochemistry 21*:4989–4999.
Matthews CR. 1991. The mechanism of protein folding. *Curr Opin Struct Biol 1*:28–35.
Mui PW, Konishi Y, Scheraga HA. 1985. Kinetics and mechanism of the refolding of denatured ribonuclease A. *Biochemistry 24*:4481–4489.
Oas T, Kim PS. 1988. A peptide model of a protein folding intermediate. *Nature 336*:42–48.
Pflumm M, Luchins J, Beychok S. 1986. Stopped flow circular dichroism. *Methods Enzymol 130*:519–534.
Ptitsyn OB. 1987. Protein folding: Hypotheses and experiments. *J Protein Chem 6*:273–293.
Ptitsyn OB, Pain RH, Semisotnov GV, Zerovnik E, Razgulyaev OI. 1990. Evidence for a molten globule state as a general intermediate in protein folding. *FEBS Lett 262*:20–24.
Radford SE, Dobson CM, Evans PA. 1992. The folding of hen egg lysozyme involves partially structured intermediates and multiple pathways. *Nature 358*:302–307.
Rasper J, Kauzmann W. 1962. Volume changes in protein reactions. I. Ionization reactions of proteins. *J Am Chem Soc 84*:1711–1777.
Richards FM, Wyckoff HW. 1971. Bovine pancreatic ribonuclease. *The Enzymes 4*:647–806.
Roder H, Elove GA, Englander W. 1988. Structural characterization of folding intermediates in cytochrome *c* by H-exchange labeling and proton NMR. *Nature 335*:700–704.
Schmid FX. 1981. A native-like intermediate on the ribonuclease A folding pathway. *Eur J Biochem 114*:105–109.
Schmid FX. 1983. Mechanism of folding of ribonuclease-A. Slow refolding is a sequential reaction via structural intermediates. *Biochemistry 22*:4690–4696.
Schmid FX. 1986. Proline isomerization during refolding of ribonuclease-A is accelerated by the presence of folding intermediates. *FEBS Lett 198*:217–220.
Schmid FX, Baldwin RL. 1978. Acid catalysis of the formation of the slow-folding species of RNase-A: Evidence that the reaction is proline isomerization. *Proc Natl Acad Sci USA 75*:4764–4768.
Schmid FX, Blaschek H. 1981. A native-like intermediate on the ribonuclease A folding pathway 2. Comparison of its properties to native ribonuclease A. *Eur J Biochem 114*:111–117.
Schmid FX, Grafl R, Wrba A, Beintema JJ. 1986. Role of proline peptide bond isomerization in unfolding and refolding of ribonuclease. *Proc Natl Acad Sci USA 83*:872–876.
Schultz DA, Baldwin RL. 1992. *Cis* proline mutants of ribonuclease A. I. Thermal stability. *Protein Sci 1*:910–916.
Schultz DA, Schmid FX, Baldwin RL. 1992. *Cis* proline mutants of ribonuclease-A. II. Elimination of the slow-folding form by mutation. *Protein Sci 1*:917–924.
Sears DW, Beychok S. 1973. Circular dichroism. In: Leach SJ, ed. *Physical principles and techniques of protein chemistry, part C*. New York: Academic Press. pp 445–593.
Sela M, Anfinsen CB. 1957. Some spectrophotometric and polarimetric experiments with ribonuclease. *Biochim Biophys Acta 24*:229–235.
Staley JP, Kim PS. 1990. Role of a subdomain in the folding of bovine pancreatic trypsin inhibitor. *Nature 344*:685–688.
Strickland EH. 1972. Interactions contributing to the tyrosyl circular dichroism bands of ribonuclease S and A. *Biochemistry 11*:3465–3474.
Strickland EH. 1974. Aromatic contributions to circular dichroism spectra of proteins. *CRC Crit Rev Biochem 2*:113–175.
Sugawara T, Kuwajima K, Sugai S. 1991. Folding of staphylococcal nuclease A studied by equilibrium and kinetic circular dichroism spectra. *Biochemistry 30*:2698–2706.
Tanford C, Kirkwood JG. 1957. Theory of protein titration curves I. General equations for impenetrable spheres. *J Am Chem Soc 79*:5333–5339.
Texter FL, Spencer DB, Rosenstein R, Matthews CR. 1992. Intramolecular catalysis of a proline isomerization reaction in the folding of dihydrofolate reductase. *Biochemistry 31*:5687–5691.
Udgaonkar JB, Baldwin RL. 1988. NMR evidence for an early framework intermediate on the folding pathway of ribonuclease-A. *Nature 335*:694–699.
Ulrich DV, Kupke DW, Beams JW. 1964. An improved magnetic densitometer: The partial specific volume of ribonuclease. *Proc Natl Acad Sci USA 52*:349–356.
von Hippel PH, Wong KY. 1965. On the conformational stability of glob-

ular proteins: The effects of various electrolytes and nonelectrolytes on the thermal ribonuclease transition. *J Biol Chem 240*:3909–3923.
Weber G, Tanaka F, Okamoto BY, Drickamer HG. 1974. The effect of pressure on the molecular complex of isoalloxazine and adenine. *Proc Natl Acad Sci USA 71*:1264–1266.
Wilkins JA, Cone J, Randhawa ZI, Wood D, Warren MK, Witowska HE. 1993. A study of intermediates involved in the folding pathway for recombinant human macrophage colony-stimulating factor (M-CSF): Evidence for two distinct folding pathways. *Protein Sci 2*:244–254.
Wyckoff HW, Tsernoglou D, Hanson AW, Knox JR, Lee BK, Richards FM. 1970. The three dimensional structure of ribonuclease-S: Interpretation of an electron density map at a nominal resolution of 2 Å. *J Biol Chem 245*:305–328.
Yang JT, Wu CSC, Martinez HM. 1986. Calculation of protein conformation from circular dichroism. *Methods Enzymol 130*:208–269.
Ybe JA. 1991. Volume changes of ribonuclease-A renaturation: Structure–volume relationships [thesis]. New Brunswick, New Jersey: Rutgers University.
Zipp A, Kauzmann W. 1973. Pressure denaturation of metmyoglobin. *Biochemistry 12*:4217–4228.
Zwanzig R, Szabo A, Bagchi B. 1992. Levinthal's paradox. *ProcNatl Acad Sci USA 89*:20–22.

Forthcoming Papers

Helix propensities of the amino acids measured in alanine-based peptides without helix-stabilizing side-chain interactions

A. Chakrabartty, T. Kortemme, and R.L. Baldwin

Crystal structures of pheasant and guinea-fowl egg-white lysozymes

J. Lescar, H. Souchon, and P.M. Alzari

Crystal structure of recombinant human triosephosphate isomerase at 2.8 Å resolution: Triosephosphate isomerase-related human genetic disorders and comparison with the trypanosomal enzyme

S.C. Mande, V. Mainfroid, K.H. Kalk, K. Goraj, J.A. Martial, and W.G.J. Hol

Structure of glutathione reductase from *Escherichia coli* at 1.86 Å resolution: Comparison with the enzyme from human erythrocytes

P.R.E. Mittl and G.E. Schulz

A conserved glutamic acid bridge in serine carboxypeptidases, belonging to the α/β hydrolase fold, acts as a pH-dependent protein stabilizing element

U.H. Mortensen and K. Breddam

Conserved phosphorylation of serines in the Ser-X-Glu/Ser(P) sequences of the vitamin K-dependent matrix Gla protein from shark, lamb, rat, cow, and human

P.A. Price, J.S. Rice, and M.K. Williamson

Comparison of the structures and the crystal contacts of trypanosomal triosephosphate isomerase in four different crystal forms

K.V. Radha Kishan, J.Ph. Zeelen, M.E.M. Noble, T.V. Borchert, and R.K. Wierenga